

Hydrated Cr(V) Peroxychromates $M_3CrO_8 \cdot xH_2O$ ($M = Li, Na, Cs$): Model $3d^1$ Systems Exhibiting Linear Chain Behavior and Antiferromagnetic Interactions

Brant Cage,[†] William Geyer,[†] Khalil A. Abboud,[‡] and Nar S. Dalal^{*,†}

Department of Chemistry and National High Magnetic Field Laboratory, Florida State University, Tallahassee FL, 32306-4390, and Department of Chemistry, University of Florida, Gainesville, Florida, 32611

Received August 11, 2000. Revised Manuscript Received December 15, 2000

A new class of Cr(V) peroxychromates, those containing waters of hydration ($Li_3CrO_8 \cdot 10H_2O$, $Na_3CrO_8 \cdot 14H_2O$ and $Cs_3CrO_8 \cdot 3H_2O$), has been synthesized and characterized by single-crystal X-ray diffraction, magnetic susceptibility, specific heat, and EPR techniques. The Li salt crystallizes into the orthorhombic ($Cmcm$) group, whereas the Na and Cs salts exhibit the triclinic ($P\bar{1}$) and monoclinic $P2(1)/n$ space groups, respectively. Crystal structure analysis indicated the availability of low-dimensional spin-exchange pathways. The orientation dependence of the EPR line width exhibited the $(3 \cos^2 \theta - 1)^{4/3}$ behavior characteristic of linear chain compounds, with $\theta = 0$ coinciding with the chain axis. Correlation of the EPR and X-ray data allowed for the explicit determination of the magnetic chain axes in the crystal and molecular frameworks. Magnetic susceptibility, χ , measurements on oriented single crystals yielded negative values for the Curie–Weiss temperatures, indicating dominant antiferromagnetic interactions. The χ data yielded the Curie constants that appear to be inversely related to the number of waters of hydration in the crystal structure; this observation is not yet understood. Correlation of the EPR line width, nearest neighbor distances, and Curie constants attested to the essential correctness of the linear chain spin exchange and dipolar fields in the Li and Cs salts, and to a lesser extent also for the Na salt. The specific heat data indicated that all these compounds have the potential to be useful for devices requiring strong heat sinks as well as magnetic refrigerants in the 250 mK temperature regime. They appear to be good as model systems for theoretical investigations on low-dimensional magnetic lattices and for understanding aspects of Cr(VI)-based catalysis and carcinogenesis.

I. Introduction

Compounds based on Cr(V) ion are among the simplest magnetic systems since they can be described by the simple $S = 1/2$ spin Hamiltonian. This is because the orbital angular momentum is largely quenched due to crystal-field effects; hyperfine effects are essentially absent because the dominant isotopes ($^{50,52,54}Cr$) all have nuclear spin $I = 0$, and there is no zero-field (D) term. It is, therefore, desirable that new Cr(V) compounds be developed since they can serve as model systems for theoretical as well as experimental studies in magnetism. Additionally, chromium in the hexavalent state has been identified as a carcinogen and the magnetic and spectroscopic properties^{1–3} of Cr(V) and Cr(IV) provide a means of detection for intermediates in the carcinogenic cycle. Also, Cr(V) has been proposed⁴ to be

the active site in the catalytic dehydrogenation of propane, indicating a broad role for this ion.

While Cr(V) compounds were initially described by Riesenfeld⁵ in 1905, spectroscopic and magnetic investigations using crystals were first reported⁶ on K_3CrO_8 in 1981. Further structural, EPR spectroscopic, and thermomagnetic studies of K_3CrO_8 and its analogues Na_3CrO_8 and Rb_3CrO_8 have been reported recently.^{7,8} These latter studies^{7,8} showed that the peroxychromates exhibit unusual short-range magnetic ordering, phase transitions, and specific heat behavior in the liquid 3He temperature region. These results encouraged us to investigate other forms of Cr(V). In particular, in a recent EPR study of the identification of Cr(V) intermediates formed in the reaction of H_2O_2 on Na_2CrO_4 in relationship to the mechanism of Cr(VI)-induced carcinogenesis, Zhang and Lay² have suggested that in solution the Cr(V)-peroxo ion may exist in hydrated as

* To whom correspondence should be addressed. E-mail: dalal@chem.fsu.edu.

[†] Florida State University.

[‡] University of Florida.

(1) Chiu, N.; Shi, X.; Beaubier, J.; Dalal, N. S. *Environ. Carcinog. Ecotoxicol. Rev.* **1998**, C16, 135–48.

(2) Zhang L.; Lay, P. A. *Inorg. Chem.* **1998**, 37, 1729–33.

(3) Cage, B.; Leniek, R.; Dalal, N. S. *J. Appl. Phys.* **2000**, 87, 6010–12.

(4) Zou, H. H.; Han, Y.; Ji, W.; Shen, J. *Chem. Lett.* **1999**, 8, 761–2.

(5) Riesenfeld, E. H. *Chem. Ber.* **1905**, 38, 4068.

(6) Dalal, N. S.; Millar, J. M.; Jagadeesh, M. S.; Seehra, M. S. *J. Chem. Phys.* **1981**, 74, 1916–22.

(7) Cage, B.; Singh, K.; Friedberg, S.; Shimizu, S.; Moodera, J. S.; Lawless, W. N.; Dalal, N. S. *Solid State Commun.* **2000**, 113, 93–7.

(8) Cage, B.; Dalal, N. S. *Chem. Mater.* **2001**, 13, 880–890.

Table 1. Crystal Parameters of the Peroxychromates

	compound		
	Li ₃ CrO ₈ ·10H ₂ O	Na ₃ CrO ₈ ·14H ₂ O	Cs ₃ CrO ₈ ·3H ₂ O
crystal class	orthorhombic	triclinic	monoclinic
space group	<i>Cmcm</i>	<i>P</i> $\bar{1}$	<i>P2(1)/n</i>
<i>a</i> (Å)	7.5170	7.5449	8.3793
<i>b</i> (Å)	12.1531	8.6556	11.992
<i>c</i> (Å)	16.7134	9.0016	11.506
α (°)	90	64.168	90
β (°)	90	81.599	91.546
γ (°)	90	69.329	90
nearest neighbor (Å)	7.14	7.55	7.03
chain axis	(1,0,0)	(1,0,0)	(-1,0,1)

well as nonhydrated forms. The present study supports this hypothesis and reports on the synthesis, crystal growth, X-ray structure determination, EPR, and thermomagnetic measurements of a new class of Cr(V) peroxychromates, those containing waters of hydration: Li₃CrO₈·10H₂O, Na₃CrO₈·14H₂O, and Cs₃CrO₈·3H₂O. The data show that these new compounds are distinctly different from their unhydrated^{7,8} counterparts (e.g., Na₃CrO₈, K₃CrO₈, and Rb₃CrO₈) in structural and magnetic properties, especially with regard to the enhancement of low-dimensionality spin exchange interactions.

II. Experimental Section

Synthesis and Crystal Growth. The peroxychromates were synthesized by modification of the method of Riesenfeld.⁵ In general, the synthesis involves the reduction of Cr(VI) by H₂O₂ in the appropriate base at temperatures of 5 °C. Good quality crystals are obtainable by crystallization around room temperature, rather than -15 °C.

Specifically, 20 g of CrO₃ was dissolved in 200–300 mL of an aqueous MOH (M = Li, Na, Cs) 25% solution (by weight, pH = 12–14) and cooled in an ice bath to ~5 °C. Then 40–60 mL of cold H₂O₂ was added dropwise without stirring over the course of 3 h. The black red solution was placed in the refrigerator at 5 °C for 3–5 days. Growth by slow evaporation produced dark red crystals of typical 1 × 1 × 3 mm³ or longer size. Appendix A provides the shapes for the Li and Cs salts. A preliminary account has been published earlier.^{7,8}

Crystal Structure. The crystal structures were determined at 173 K using a Siemens SMART PLATFORM. Table 1 provides a summary of the observed crystal parameters. Atomic coordinates are available from the authors and will be deposited with the Cambridge database. The relations of the crystal morphologies to the crystal axes for the Li and Cs salts are given in Appendix A.

Specific Heat Measurements. Heat capacity was measured between 1.8 and 10 K on single-crystal samples (~2–3 mg) using a Quantum Design Physical Properties Measurement System (QD PPMS) employing a time constant⁹ method. The platform was calibrated using a copper standard.¹⁰

Magnetic Measurements. dc magnetic susceptibility (χ) measurements were made using a Quantum Design SQUID magnetometer in the temperature range of 1.8–20 K at a magnetic field of 3000 Gauss (G) (10 000 G = 1 Tesla (T)) using oriented single crystals.

EPR Measurements. Angular-dependent EPR line width measurements were made at X-band (~9.5 GHz) using a Varian E-12 spectrometer. The crystals were oriented with respect to the applied magnetic field by use of a homemade goniometer. The microwave frequency was measured with a

Hewlett-Packard (model 5340A) digital frequency counter. Parameters of the *g* tensor were obtained at the *W*band (~95 GHz) frequency using a homemade microwave bridge and a Quantum Design 9 T PPMS magnet. The frequency was measured with an EIP model 578B source locking microwave counter. The magnetic fields were calibrated using DPPH and also 0.5% K₃CrO₈ diluted into a diamagnetic K₃NbO₈ matrix, as discussed elsewhere.¹¹ All measurements were performed at room temperature.

III. Investigations on the Hydrated Peroxychromates Li₃CrO₈·10H₂O, Cs₃CrO₈·3H₂O, and Na₃CrO₈·14H₂O

As expected, the cations Li, Na, and Cs resulted in the formation of hydrated lattices with varying degrees of hydration. X-ray diffraction studies on the Li and Cs salts establish the formulas as Li₃CrO₈·10H₂O and Cs₃CrO₈·3H₂O. The Na salt was found to crystallize in both a hydrated and a nonhydrated⁸ form. The molecular formula of the hydrated lattice was determined to be Na₃CrO₈·14H₂O by X-ray diffraction.

III.A. Crystal Structures. Figures 1a and b show the cationic-water units for the Cs and Li salts, respectively. Li₃CrO₈·10H₂O crystallizes in the space group *Cmcm* with *z* = 4 (where *z* is the number of Cr(V) ions/unit cell). The unit cell is orthorhombic and the cell dimensions are *a* = 7.5170, *b* = 12.1531, and *c* = 16.7134 Å. Figure 2 presents the lattice of the Li salt (waters are omitted for clarity); there exist alternating sheets of CrO₈³⁻ and Li⁺ ions in the *ab* plane. The nearest neighbor, NN, (Cr–Cr) distance (*r*) is 7.14 Å; however, further analysis of the structure indicates that the shortest super-exchange pathway involving Cr–O–O–Cr (1.93, 3.66, and 1.93 Å) is along the *a* axis to the second NN, where *r* = 7.52 Å. Therefore, the crystal structure suggests that magnetic exchange should be preferential along the *a* axis. This will be further discussed in relationship to EPR line width results in section V.

Cs₃CrO₈·3H₂O forms a monoclinic lattice with the space group *P2(1)/n*. The unit cell parameters are *a* = 8.3793 Å, *b* = 11.9915 Å, *c* = 11.5060 Å, and *z* = 4. A projection along the (0,1,0) axis is shown in Figure 3. The NNs are spaced 7.032 Å along the (-1,0,1) axis, indicating that this may be the preferred chain axis. This also will be compared to EPR results, *vide infra*.

Na₃CrO₈·14H₂O crystallizes in the space group *P* $\bar{1}$, the symmetry is triclinic, and the unit cell parameters are *a* = 7.5449 Å, *b* = 8.6556 Å, *c* = 9.0016 Å, α = 64.168°, β = 81.599°, γ = 69.329°, and *z* = 1. Figure 4 presents a projection down the *b* axis, where the waters are omitted for clarity. The NN (by more than an Å) lie along the *a* axis, suggesting this may be the chain axis, as indicated by the arrow.

The crystal parameters for all three compounds are summarized in Table 1.

III.B. Magnetic Susceptibility of Oriented Crystals of Li₃CrO₈·10H₂O, Na₃CrO₈·14H₂O, and Cs₃CrO₈·3H₂O. We measured magnetic susceptibilities using oriented single crystals of Li₃CrO₈·10H₂O, Cs₃CrO₈·3H₂O, and Na₃CrO₈·14H₂O. These measurements encompassed two orthogonal orientations with respect to the applied field. No phase transitions were observed

(9) For a review of low-temperature calorimetry, see Stewart, G. R. *Rev. Sci. Instrum.* **1983**, *54*, 1–11.

(10) Leyarovski, E. I.; Leyarovska, L. N.; Popov, O. *Cryogenics* **1987**, *28*, 321–35.

(11) Cage, B.; Weekley, A.; Brunel, L.-C.; Dalal, N. S. *Anal. Chem.* **1999**, *71*, 1951–7.

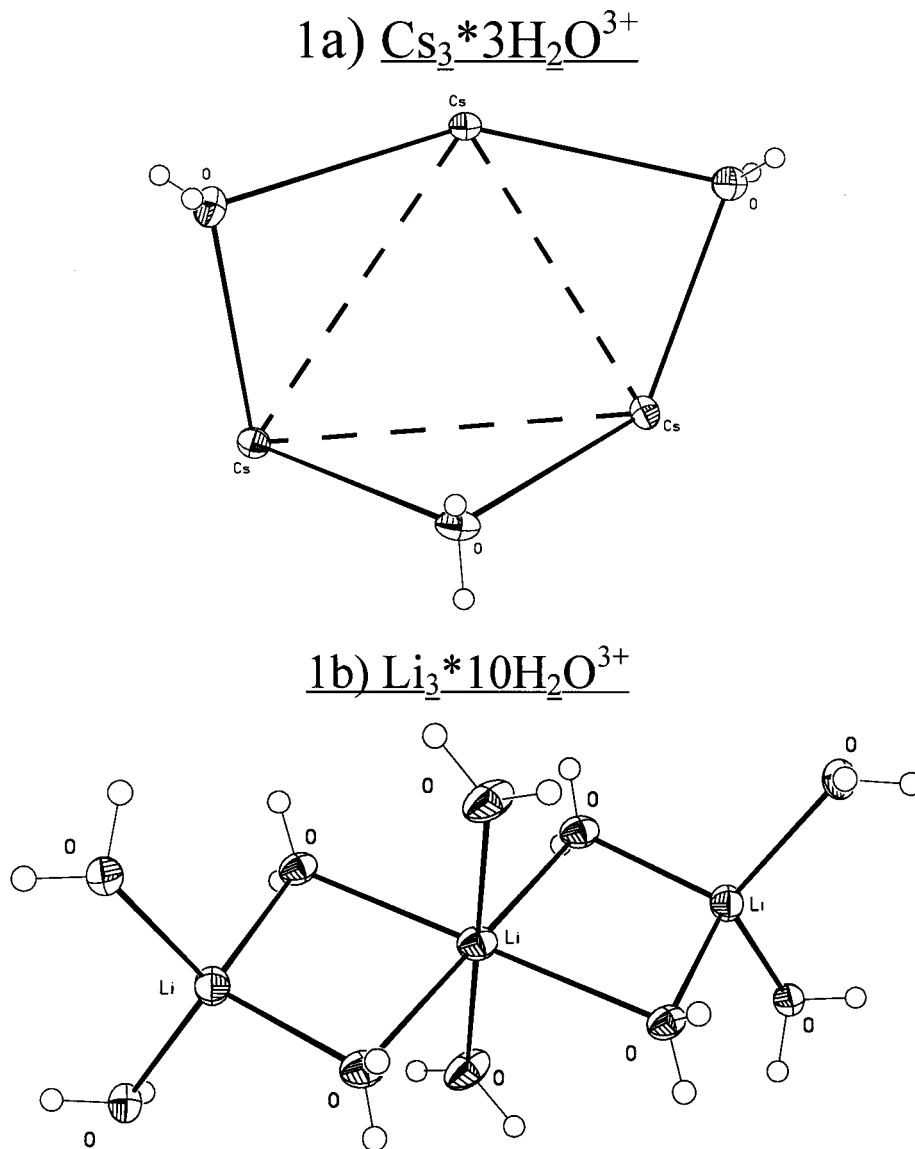


Figure 1. Depictions of the (a) $\text{Cs}_3 \cdot 3\text{H}_2\text{O}^{3+}$ and (b) $\text{Li}_3 \cdot 10\text{H}_2\text{O}^{3+}$ units.

down to 1.8 K, and χ was observed to be independent of the fields at the temperatures used in this investigation. Figure 5 shows a plot of $1/\chi$ vs temperature (T) in the low-temperature range from which the Curie constants (inverse slope (C)) and Curie–Weiss temperatures (χ intercept (θ)) were obtained in a manner previously outlined.^{6,8} These are presented in Table 2. The negative values of θ obtained for all cases imply the magnetic exchange for the hydrated peroxychromates is antiferromagnetic in nature, just as in the case of the unhydrated lattices.⁸ The χ data were complemented by specific heat measurements, as described next.

III.C. Specific Heat (C_p) Measurements. Figure 6 shows the temperature dependence of C_p for all three lattices, and the data are interpreted as follows. For an insulating paramagnet the main contributions to the heat capacity in the low-temperature region can be described by¹²

$$C = \alpha T^3 + bT^{-2} \quad (1)$$

where α and b are parameters to be fitted. The cubic term represents the lattice contribution, and the inverse

squared term represents the high-temperature limit of the magnetic heat capacity. Figure 7 presents a plot of C_p/T^3 vs T^{-5} . A linear relationship is observed whereby the parameters b (slope) and α (y intercept) were obtained, as listed in Table 2. The b parameter or magnetic heat capacity coefficient is important as a measure of the available entropy,¹³ and as a barometer of the magnetic refrigeration potential, which is discussed in section VI.

In agreement with χ , no phase transitions were observed down to 1.8 K. This is both expected and consistent with previous⁸ work on the nonhydrated forms of the peroxychromates where the relationship between the Cr–Cr distance, (r), along the chain axis and the exchange energy (J) was found to be

$$|J|/k = -0.076 \text{ K} + (2.65 \exp(-(r - 5.53 \text{ \AA})/0.72 \text{ \AA})) \text{ K} \quad (2)$$

(12) Carlin R. L.; Van Duijneveldt, A. J. *Magnetic Properties of Transition Metal Compounds*; Springer-Verlag: New York, 1977; pp 25, 56–62, 123.

(13) Abraham, B. M.; Ketterson J. B.; Roach, P. R. *J. Low Temp. Phys.* **1974**, *14*, 387–96.

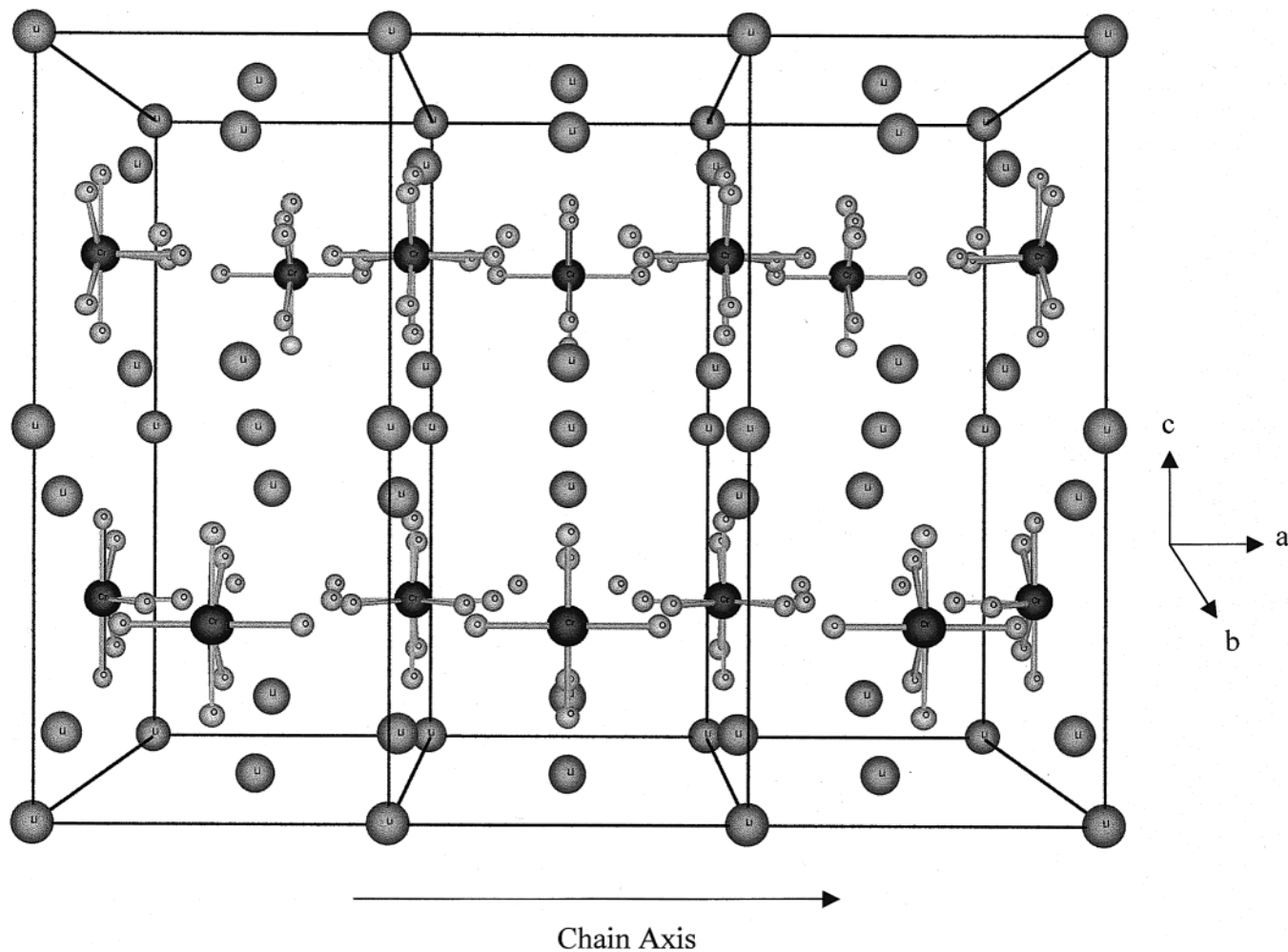


Figure 2. Crystal lattice of $\text{Li}_3\text{CrO}_8 \cdot 10\text{H}_2\text{O}$ (waters omitted for clarity). Analysis indicates the minimum distance for a superexchange pathway, $\text{Cr}-\text{O}-\text{O}-\text{Cr}$, lies along the a axis, as indicated by the arrow. Angular dependence of the EPR line width confirms that the $(1,0,0)$ axis is indeed the magnetic chain axis.

Use of eq 2 and $\text{Cr}-\text{Cr}$ distance of 7.5 \AA predicts that the exchange energies of the hydrated peroxochromates should be $\sim 250 \text{ mK}$, well below the temperature range investigated.

However, if the behavior of C_p of the hydrated peroxochromates is similar to that of the nonhydrated peroxochromates,⁸ then there may exist large, broad, Bonner–Fisher¹⁴ like peaks in the heat capacity in the temperature region of $\sim 250 \text{ mK}$ or less. This will be discussed in section VI in the context of their possible application as heat sinks, *vide infra*.

IV. EPR Determination of the Electronic Ground State

The ground state of the lone $3d^1$ electron of the CrO_8^{3-} ion can be easily determined using EPR spectroscopy.^{6,15} The hybridization⁶ of the peroxochromates has been shown to be d^4sp^3 with the unpaired electron residing in either the d_{z^2} orbital or the $d_{x^2-y^2}$ orbital. The ground

states of the nonhydrated salts have been previously determined⁸ and we follow the same procedure here for the hydrated salts.

As a typical example, the EPR spectrum of $\text{Li}_3\text{CrO}_8 \cdot 14\text{H}_2\text{O}$ powder at the W band ($\sim 95 \text{ GHz}$) is presented in Figure 8. The spectrum results from the Zeeman interaction of the $3d^1$ unpaired electron on the $^{50,52,54}\text{Cr}$ (90.5% natural abundance) isotopes. Thus, to a good approximation there is no hyperfine interaction expected, and the spectrum should reflect peaks at the principal values of the \mathbf{g} tensor for each compound. For a lattice with tetragonal symmetry, we thus expect the spectrum to exhibit only two peaks¹⁶ in the first-derivative presentation: one corresponding to the resonance absorption of molecules whose tetragonal axis is oriented along the Zeeman field (labeled g_{\parallel}) and the other absorption from those molecules whose tetragonal axis is aligned perpendicular to the field direction

(14) Bonner, J. C.; Fisher, M. E. *Phys. Rev.* **1964**, *135*, 3A, 640–58.

(15) McGarvey, B. R. *Electron Spin Resonance of Metal Complexes*; Yen, T. F., Ed.; Plenum Press: New York, 1969; pp 1–11.

(16) Li salt possesses orthorhombic symmetry and may be expected to exhibit three peaks in the EPR spectrum corresponding to the three canonical orientations of the \mathbf{g} tensor, g_{xx} , g_{yy} , and g_{zz} . However, even at the W band, the g_{yy} and g_{zz} peaks were not resolved. One might expect that at higher microwave frequencies three peaks could be observed. Further studies at still higher frequencies should be fruitful.

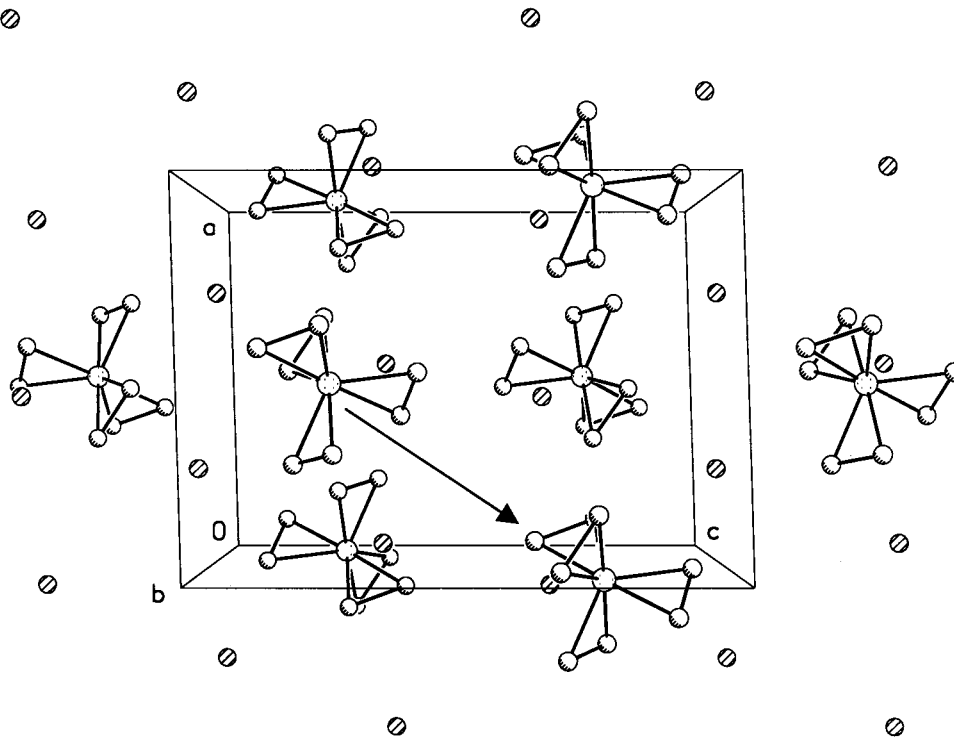


Figure 3. Projection down the b axis of $\text{Cs}_3\text{CrO}_8 \cdot 3\text{H}_2\text{O}$ (waters omitted, solid = O, stripes = Cs, dotted = Cr). The arrow indicates magnetic chain axis, as determined from EPR, coinciding with the NN, as determined by X-ray diffraction.

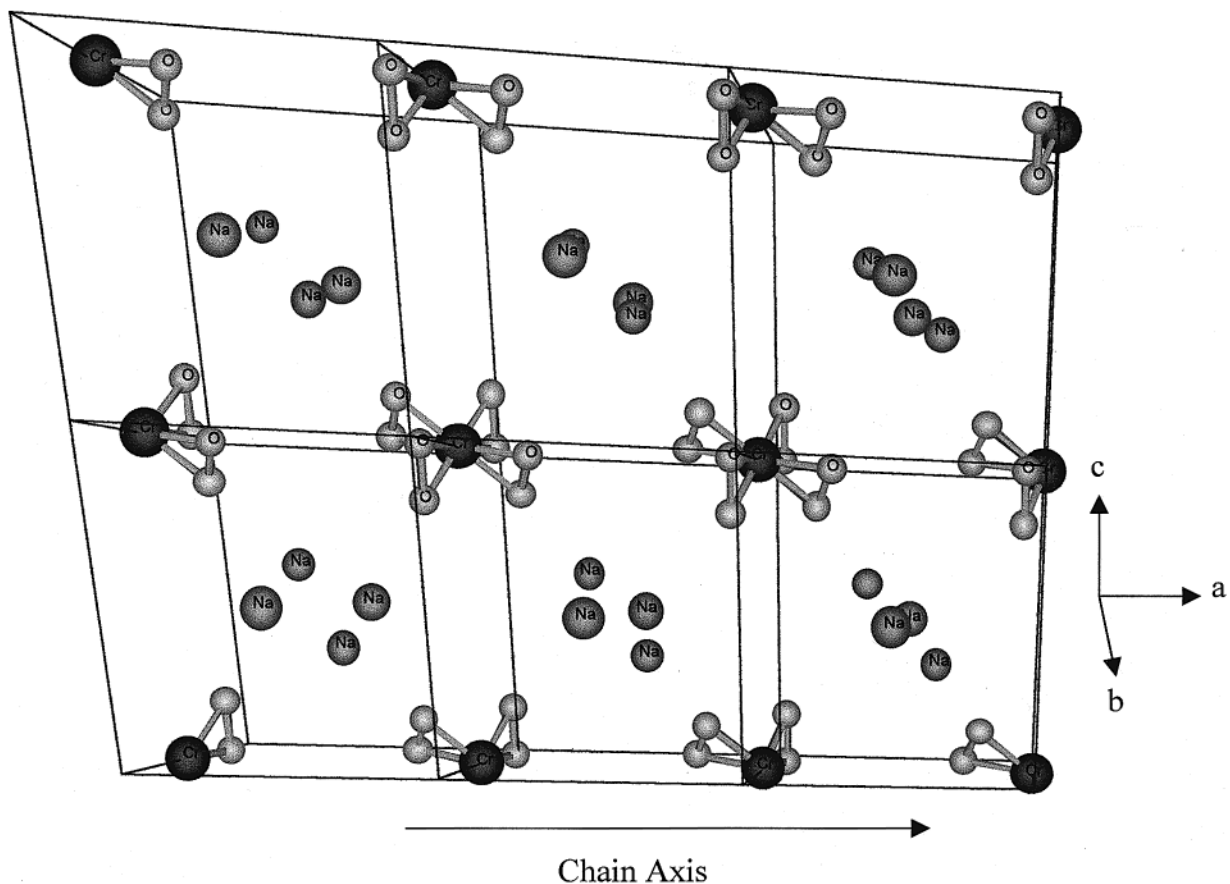


Figure 4. $\text{Na}_3\text{CrO}_8 \cdot 14\text{H}_2\text{O}$ projected down the b axis. EPR indicates that linear chains are present, and the crystal structure suggests these chains are along the NN down the a axis as shown by the arrow.

(labeled g_{\perp}). At the W -band frequency the spectrum becomes highly resolved. It is easily determined that $g_{\perp} > g_{\parallel}$ and the ground state to be $d_{x^2-y^2}$.

Similar results were obtained for the Na and Cs salts and the g values and ground states are listed in Table 3.

Table 2. Magnetic Parameters of the Hydrated Peroxychromates^a

compound	$-\theta_{\perp}$ (K)	$-\theta_{\parallel}$ (K)	C_{\perp} (emu·K/mol)	C_{\parallel} (emu·K/mol)	b (J·K/mol)	α (J/(K ⁴ ·mol))
Li ₃ CrO ₈ ·10H ₂ O	0.40	0.37	0.286 ± 0.005	0.279 ± 0.005	0.36	0.0037
Na ₃ CrO ₈ ·14H ₂ O	0.17	0.06	0.251 ± 0.005	0.222 ± 0.005	<10 ⁻²	0.034
Cs ₃ CrO ₈ ·3H ₂ O	0.27	0.40	0.361 ± 0.005	0.345 ± 0.005	0.48	0.0059

^aNote: Orientations are with respect to the c axis; all least-squares-fits for C had a correlation factor ≥ 0.9999 .

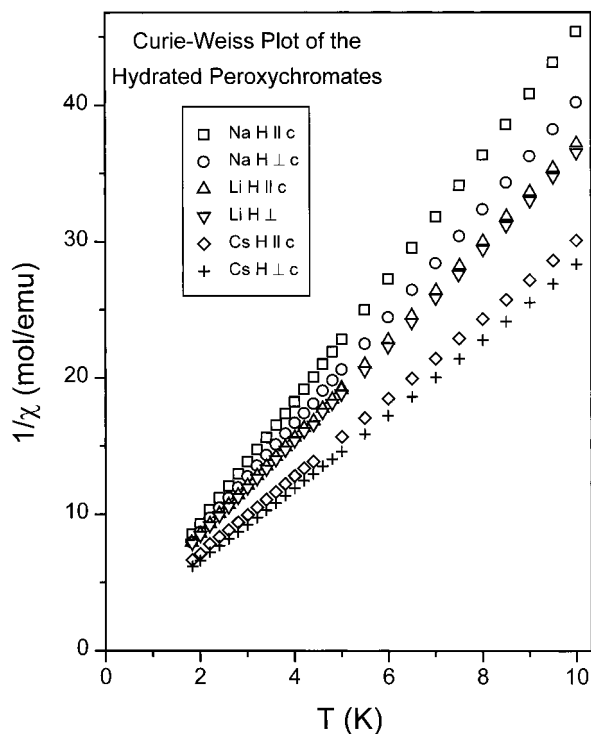


Figure 5. Temperature dependence of χ^{-1} for the three peroxychromate salts. The crystal's c axes are oriented parallel and perpendicular to the Zeeman field.

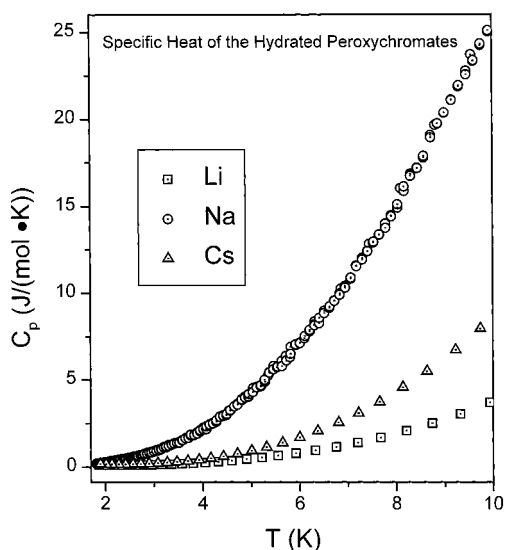


Figure 6. Temperature dependence of the specific heat for the three peroxychromate salts of Li, Na, and Cs.

V. EPR Evidence for Low-Spin Dimensionality

It is well-known that EPR spectroscopy could provide direct evidence for low-spin dimensionality of the spin exchange.¹⁷⁻¹⁹ It has been shown that the angular

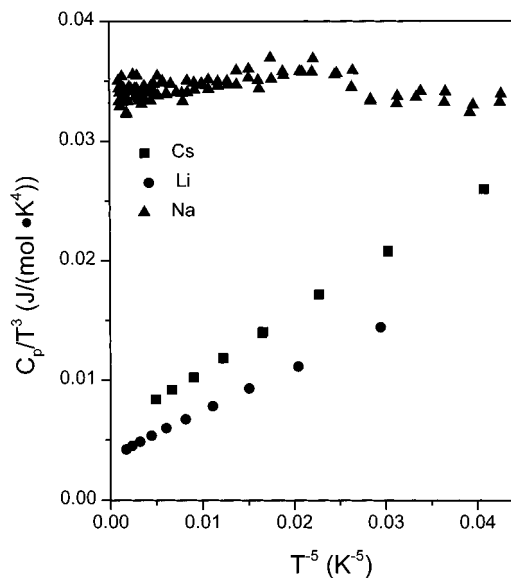


Figure 7. Plot of $C_p T^{-3}$ vs T^{-5} for the three hydrated peroxychromate salts, Li, Na, and Cs. From this plot we obtained the magnetic heat capacity coefficient, b (slope), and the Debye cube law constant, α (y intercept). The low magnitude of the slope for the Na salt indicates it may have potential as a magnetic refrigerant.

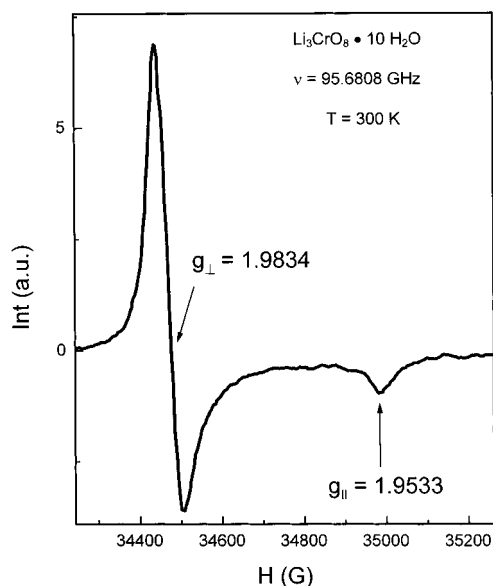


Figure 8. W band (95.6808 GHz) EPR spectrum (room temperature) of powdered Li₃CrO₈·10H₂O. Notice that $g_{\perp} > g_{\parallel}$, proving the ground state to be $d_{x^2-y^2}$.

dependence of the EPR peak-to-peak line width, ΔH_{pp} , for a one-dimensional system is¹⁷⁻¹⁹

$$\Delta H_{pp} = A + B|3 \cos^2 \theta - 1|^{4/3} \quad (3)$$

where the constant A is representative of the residual

Table 3. g Values and Electronic Ground States of the Hydrated Peroxychromates^a

compound (resonant field ~ 3.4 T)	$g_z (\pm 0.0005)$	$g_y (\pm 0.0005)$	$g_x (\pm 0.0005)$	electronic ground state	A (G)	B (G)
$\text{Na}_3\text{CrO}_8 \cdot 14\text{H}_2\text{O}$	(a) 1.9476 (b) 1.9539	(a) 1.9821 (b) 1.9834		$d_{x^2-y^2}$	28	12
$\text{Li}_3\text{CrO}_8 \cdot 10\text{H}_2\text{O}$	1.9533	1.9834		$d_{x^2-y^2}$	7.7	3
$\text{Cs}_3\text{CrO}_8 \cdot 3\text{H}_2\text{O}$	1.9546	1.9702	1.9817	$d_{x^2-y^2}$	12.5	1.5

^a Note: The parallel and perpendicular features of $\text{Na}_3\text{CrO}_8 \cdot 14\text{H}_2\text{O}$ were observed to split into doublets at the W band (95 GHz); this is attributed to powdering effects and dehydration.

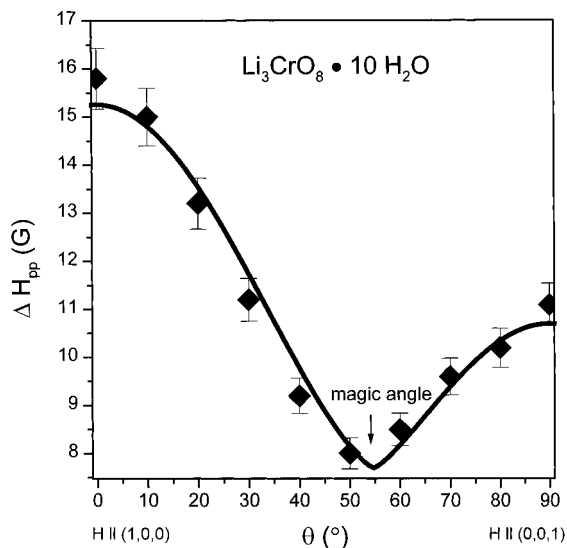


Figure 9. Angular variation of the peak-to-peak EPR line width (room temperature) upon rotation from the a axis to the c axis of $\text{Li}_3\text{CrO}_8 \cdot 10\text{H}_2\text{O}$. The drawn line is a fit using eq 3, in agreement with the experimental data. There is observed a marked minimum at the magic angle, indicating that the magnetic exchange is of a chainlike nature and that (1,0,0) is the magnetic chain axis.

line width as determined by spin–lattice relaxation, and other lifetime processes, B is representative of the secular dipolar terms, and θ is the angle between the chain axis and the Zeeman field. This relationship is characterized by a sharp minimum in the line width at the magic angle of $\theta \sim 54.7^\circ$, when the secular components go to zero. In contrast, for the case of three-dimensional exchange,²⁰ the line width is proportional to $(1 + \cos^2 \theta)$, which exhibits a broad minimum at $\theta \sim 90^\circ$.

Figure 9 shows the angular dependence of the EPR line width upon rotation from the (1,0,0) axis to the (0,0,1) axis for the Li salt. There exists a marked angular dependence with a minimum within experimental error of the magic angle. The solid line is a fit using eq 3 with $A = 7.7$ G and $B = 3$ G, in agreement with the experimental data. This result was briefly reported earlier,⁷ but at that time the crystal structure had not been determined and no mention was made of the waters of hydration. The crystal analysis supports low-dimensional magnetic exchange along the a axis, as evidenced in Figure 2, and discussed in section III. A. Appendix A allows the determination from EPR that, indeed, the magnetic chain axis coincides with the

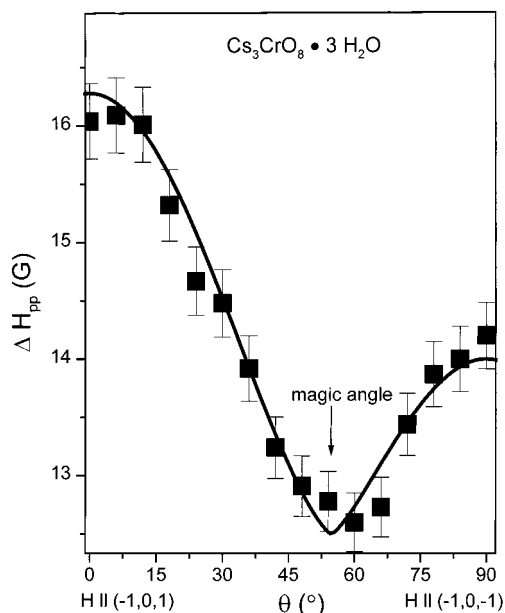


Figure 10. Angular variation of the peak-to-peak EPR line width (room temperature) of $\text{Cs}_3\text{CrO}_8 \cdot 3\text{H}_2\text{O}$. The drawn line is a fit using eq 3, in agreement with the experimental data, indicating that (–1,0,1) is the magnetic chain axis.

crystal a axis. Therefore, both structural and EPR data are consistent with a linear chain model.

Figure 10 shows a plot of ΔH_{pp} vs θ (where $\theta = 0^\circ$ corresponds to the (–1,0,1) axis) for $\text{Cs}_3\text{CrO}_8 \cdot 3\text{H}_2\text{O}$. Again, there exists a marked angular dependence with a minimum within experimental error of the magic angle. The fit to eq 3 (solid line) yielded $A = 12.5$ G and $B = 1.5$ G. This result demonstrates that $\text{Cs}_3\text{CrO}_8 \cdot 3\text{H}_2\text{O}$ is a linear chain electron exchange compound and the (–1,0,1) direction corresponds to the chain axis. Figure 3 shows a projection down the b axis. The Cr ions form chains (indicated by the arrow) separated 7.03 Å from their NN. As before, use of Appendix A and EPR showed that the magnetic chain axis coincides with the crystal (–1,0,1) axis.

Similar results have been observed for $\text{Na}_3\text{CrO}_8 \cdot 14\text{H}_2\text{O}$, as shown in Figure 11. A clear minimum is present at the magic angle. The solid line is a fit to eq 3, resulting in $A = 28$ G and $B = 12$ G, the largest observed of the three investigated salts.

The line width dependence of J and r , for one-dimensional systems²¹ at $\theta = 0^\circ$ is

$$\Delta H_{pp} \propto |J|^{-1/3} r^{-4} \quad (4)$$

so $\Delta H_{pp}|J|^{1/3}r^4$ should be similar for all three compounds. We start with the high crystal quality salts, these of Cs and Li. The product of ΔH_{pp} , $J^{1/3}$, and r^4 agrees to within $\sim 3\%$ using θ (Table 2) as a relative approximation for

(17) Bencini, A.; Gatteschi, D. *EPR of Exchange Coupled Systems*; Springer-Verlag: New York, 1990; p 135.

(18) Dietz, R. E.; Meritt, F. R.; Dingle, R.; Hone, D.; Silbernagel, B. G.; Richards, P. M. *Phys. Rev. Lett.* **1971**, *26*, 1186–9.

(19) Dalal, N. S.; Smirnov, A. I.; Smirnova, T. I.; Belford, R. L.; Katritzky, A. R.; Belyakov, S. A. *J. Phys. Chem. B* **1997**, *101*, 11249–53.

(20) Kubo, R.; Tomita, K. *J. Phys. Soc. Jpn.* **1954**, *9*, 888–919.

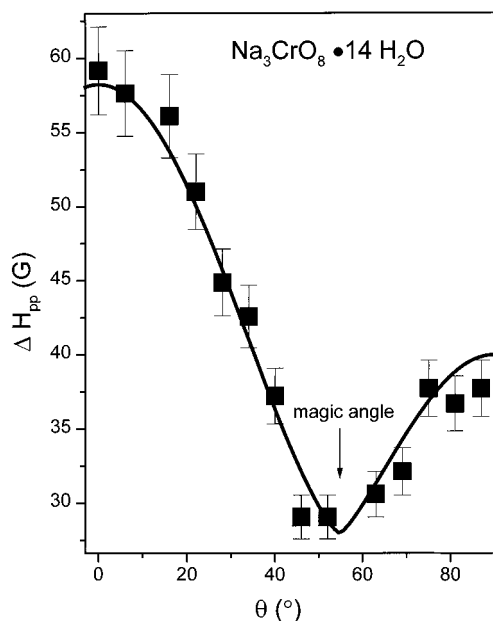


Figure 11. Angular variation of the peak-to-peak EPR line width (room temperature) of $\text{Na}_3\text{CrO}_8 \cdot 14\text{H}_2\text{O}$. Drawn line is a fit of eq 3 to the experimental data. Crystal structure indicates that these chains run along the (1,0,0) axis.

J and r as found in Table 1. The Na salt is a factor of ~ 2.5 larger, which is ascribed to inhomogeneous broadening due to lattice defects. In the Na salt, these defects may be related to differential loss of water during EPR, susceptibility, X-ray, and heat capacity measurements. Be that as it may, the simplicity of the structure and clarity of the observed data suggest that the peroxochromates might be of use as model systems for the dependence of metal-oxide exchange interactions on bond angles, interion distances, and counterions.

VI. Utility as Heat Sinks and Magnetic Refrigerants

Heat capacity data (Table 2) indicates that the hydrated peroxochromates may be valuable as heat sinks in the 250 mK or less temperature range. This is based on eq 2 using a Cr–Cr distance of ~ 7.5 Å, as explained in section III.C. Since crystal structure and EPR data indicate that the hydrated peroxochromates are low dimensional in nature, then the behavior of their C_p 's should be similar to that of the nonhydrated peroxochromates,⁸ except at lower temperatures. One may then expect broad Bonner–Fisher¹⁴ like peaks in C_p in the temperature region of ~ 250 mK. Previous work^{7,8} has shown that the magnitude of C_p at the maximum is generally in the area of 3–4 J/mol·K. If further experiments confirm this, then the hydrated peroxochromates may be used as heat sinks in the ~ 250 mK or less temperature arena.

Additionally, the peroxochromates may have value as magnetic refrigerants. This claim is based upon evaluation of the heat capacity coefficient (b), which is derived from the high-temperature behavior of the magnetic

specific heat (C_m) such that $C_m = b/T^2$. It is known that the lower the magnitude of b , the greater the realization of the total refrigeration potential.^{12,22} Our earlier analysis²² indicates that a general trend is followed whereby introducing larger cations and/or adding waters of hydration significantly lowers b , while basically maintaining the spin concentration (or refrigeration potential). The conclusion drawn is that the hydrated salts $\text{Cs}_3\text{CrO}_8 \cdot 3\text{H}_2\text{O}$ ($b = 0.48$ J·K/mol) and $\text{Li}_3\text{CrO}_8 \cdot 10\text{H}_2\text{O}$ ($b = 0.36$ J·K/mol) would be comparable magnetic refrigerants to the commonly used material chrome alum¹² ($b = 0.149$ J·K/mol) in the 300 mK to 4 K range. Figure 7 shows that the dependence of C_p/T^3 vs T^{-5} for $\text{Na}_3\text{CrO}_8 \cdot 14\text{H}_2\text{O}$ is essentially horizontal. The magnetic contribution is not detectable within the error of the measurement above 1.8 K, leading to an estimate of a b parameter of 10^{-2} J·K/mol or less. Therefore, it is predicted that $\text{Na}_3\text{CrO}_8 \cdot 14\text{H}_2\text{O}$ would be a superior refrigerant to chrom alum in the 0.3–4 K region and possibly comparable to cerium magnesium nitrate^{12,13} ($b = 5.0 \times 10^{-6}$) in the <0.3 K region.

Conclusion

Cr(V) peroxochromates can be synthesized and grown as large single crystals of $\text{Li}_3\text{CrO}_8 \cdot 10\text{H}_2\text{O}$, $\text{Na}_3\text{CrO}_8 \cdot 14\text{H}_2\text{O}$, and $\text{Cs}_3\text{CrO}_8 \cdot 3\text{H}_2\text{O}$. Their crystal structures indicate the availability of low-dimensional spin exchange pathways. Indeed, angular-dependent EPR line width measurements showed that the magnetic spin exchange processes of these hydrated Cr(V) tetraperoxides are chainlike in nature, with the chain axis being along the Cr–O–O–Cr linkage of the (1,0,0) axis for the Li salt and between the nearest neighboring Cr(V) ions along the (–1,0,1) axis for the Cs salt. The Na salt behaved similarly and the crystal structure indicated that (1,0,0) is the chain axis. All salts exhibit negative small Curie–Weiss temperatures, indicating weak antiferromagnetic interactions. A curious observation is that while the Curie constant for $\text{Cs}_3\text{CrO}_8 \cdot 3\text{H}_2\text{O}$ essentially agrees with that for an isolated $S = 1/2$ system, (0.345), those for $\text{Li}_3\text{CrO}_8 \cdot 10\text{H}_2\text{O}$ and $\text{Na}_3\text{CrO}_8 \cdot 14\text{H}_2\text{O}$ deviate significantly, being 0.279 and 0.222, for $H \parallel c$, respectively. *The origin of this seemingly inverse role for the waters of hydration is not understood at this time and needs further investigation.*

Heat capacity data have indicated that these compounds may find useful applications as magnetic refrigerants and heat sinks in the ~ 250 mK region. These characteristics coupled with their simple electronic structure renders these peroxochromates valuable as theoretical models for metal-oxide spin exchange calculations. Finally, the fact that compounds such as sodium peroxochromate form stable structures in both the unhydrated and hydrated forms might be helpful in understanding the role of Cr(V) in chromate-related carcinogenesis, wherein $\text{Na}_2\text{CrO}_4/\text{H}_2\text{O}_2$ was used as a model system.^{1,2}

Acknowledgment. This work was partially supported by the National Science Foundation (NSF) and the Research Foundation of Florida State University. KAA acknowledges the NSF and the University of

(21) Richards, P. M. *Low Dimensional Cooperative Phenomena*; Keller, H. J., Ed.; Plenum Press: New York, 1975; pp 147–69. This relationship assumes that the Zeeman field (H_z) > exchange field (H_{ex}), a condition met for $J \sim 250$ mK.

(22) Cage, B.; Dalal, N. S. *J. Appl. Phys.* **2000**, *87*, 6031–3.

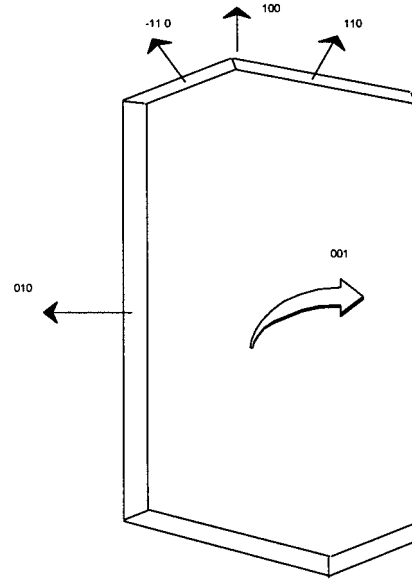
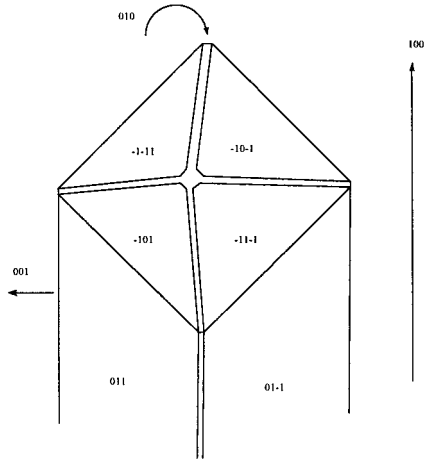
Florida for funding of the purchase of the X-ray equipment.

(2) $\text{Li}_3\text{CrO}_8 \cdot 10\text{H}_2\text{O}$

Appendix A

Relation of the crystal morphology to the crystal axes for the hydrated peroxychromates:

(1) $\text{Cs}_3\text{CrO}_8 \cdot 3\text{H}_2\text{O}$



CM0006446